AD_____

Award Number: W81XWH-12-1-0336

TITLE: Molecular Innovations Toward Theranostics of Aggressive Prostate Cancer

PRINCIPAL INVESTIGATOR: Xiankai Sun

CONTRACTING ORGANIZATION: University of Texas Southwestern Medical Center
Dallas, Texas 75390

REPORT DATE: September 2014

TYPE OF REPORT: Annual

PREPARED FOR: U.S. Army Medical Research and Materiel Command
Fort Detrick, Maryland 21702-5012

REPORT DOCUMENTATION PAGE

Form Approved
OMB No. 0704-0188

1. REPORT DATE *(DD-MM-YYYY)*	2. REPORT TYPE	3. DATES COVERED *(From - To)*
Sept 2014	Annual	1September 2013 - 31August 2014

4. TITLE AND SUBTITLE
Molecular Innovations Toward Theranostics of Aggressive Prostate Cancer

5a. CONTRACT NUMBER

5b. GRANT NUMBER
W81XWH-12-1-0336

5c. PROGRAM ELEMENT NUMBER

6. AUTHOR(S)

Xiankai Sun

email: xiankai.sun@utsouthwestern.edu

5d. PROJECT NUMBER

5e. TASK NUMBER

5f. WORK UNIT NUMBER

7. PERFORMING ORGANIZATION NAME(S) AND ADDRESS(ES)

University of Texas Southwestern Medical Center

Dallas, Texas 75390

8. PERFORMING ORGANIZATION REPORT NUMBER

9. SPONSORING / MONITORING AGENCY NAME(S) AND ADDRESS(ES)
U.S. Army Medical Research and Materiel Command
Fort Detrick, Maryland 21702-5012

10. SPONSOR/MONITOR'S ACRONYM(S)

11. SPONSOR/MONITOR'S REPORT NUMBER(S)

12. DISTRIBUTION / AVAILABILITY STATEMENT

Approved for public release; distribution unlimited

13. SUPPLEMENTARY NOTES
N/A

14. ABSTRACT: In this project, we propose to develop a new drug delivery vehicle based on dendrimer nanotechnology for personalized medicine. This new class of nanoplatforms contains imaging probe and molecular medicine with a cancer-specific targeting capability which is able to target cancer cells, monitor drug delivery and tumor response to achieve a "see and treat" strategy as a new concept of molecular medicine. Specifically, One Partner PI's lab will make dendrimers bearing functional handles to conjugate with chelating agents provided by the Initiating PI's lab for PET imaging and therapeutic peptides provided by another Partner PI's lab for the treatment of aggressive prostate cancer. In the 2nd year, the Initiating PI's lab has designed and synthesized three enantiopure chelator scaffolds for copper radiopharmaceuticals using a well-validated integrin $\alpha_v\beta_3$ ligand. In addition, a theranostic molecular drug conjugate (MDC) design was accomplished. Such design will be modified and incorporated into the dendrimeric platforms to accomplish further Aims in this project.

15. SUBJECT TERMS: none listed

16. SECURITY CLASSIFICATION OF:			17. LIMITATION OF ABSTRACT	18. NUMBER OF PAGES	19a. NAME OF RESPONSIBLE PERSON
a. REPORT	b. ABSTRACT	c. THIS PAGE		19	USAMRMC
unclassified	unclassified	unclassified	unlimited		19b. TELEPHONE NUMBER *(include area code)*

Table of Contents

INTRODUCTION

This project combines the recent advances in prostate cancer (PCa) research from three different labs integrated with a strong interest and dedication to develop a new molecular medicine approach towards the eventual cure of PCa. Like other cancer types, the current available therapeutic regimens for metastatic PCa are not PCa specific. With respect to PCa cells harboring various genetic alterations, the development of small molecular agents targeting these genetic defects to achieve a better therapeutic efficacy is foreseeable. In this project, we propose to develop a new drug delivery vehicle based on dendrimer nanotechnology for personalized medicine. This new class of nanoplatforms contains imaging probe and molecular medicine with a cancer-specific targeting capability which is able to target cancer cells, monitor drug delivery and tumor response to achieve a "see and treat" strategy as a new concept of molecular medicine. This platform system will be flexible to adopt any new cell targeting molecule or any therapeutic agents. Specifically, Dr. Simanek's lab will make dendrimers bearing functional handles to conjugate with chelating agents provided by Dr. Sun's lab for PET imaging and therapeutic peptides provided by Dr. Hsieh's lab for the treatment of aggressive PCa.

BODY

With the ultimate goal to generate a new class of dendrimer-based theranostic agents for aggressive PCa, we have arranged four Specific Aims as indicated in Statement of Work (SOW). Our work in the first two years focused on Tasks 1 – 3 to accomplish **Aim 1** and **Aim 2**.

To date, the initiating PI and the partner PIs have accomplished (and further extended) the goals set forth in the proposal and are now poised to further integrate the research progress for the construction and biological evaluation of the designed theranostic agents.

Aim 1: To construct dendrimer conjugates containing specific cell permeation peptides, peptide therapeutic(s) and a bifunctional chelator for PET imaging

Task 1 (Months 1 – 24): Synthesis and Characterization of Dendrimers - Scaffold Library

Please see Dr. Simanek's annual report for the progress of this Task

Task 2 (Months 1 – 12): Synthesis & Characterization of CB-TE2A-based Bifunctional Chelator
Accomplished in the 1st Year. Further work has been carried out to extend the accomplishment of Task 2. Enantiopure bifunctional chelators (BFCs) were designed for radiopharmaceuticals and their chirality effect was evaluated on integrin $\alpha_v\beta_3$ targeted agents.

Aim 2: To select potent compounds with screening systems based on specific mechanism(s) of action

Task 3 (Months 1 – 24). Selection of therapeutic peptides using high throughput assays

Please see Dr. Hsieh's annual report for the progress of this Task

Aim 3: To determine the biodistribution, pharmacokinetics, and potential cytotoxicity *in vivo*

Task 4 (Months 13 – 24): Synthetic and radio- chemistry and in vitro assay of the synthesized theranostic agents (Sun/Hsieh)

An imaging functionality has been incorporated into a drug conjugate platform containing an anticancer drug (DM1) and prostate specific membrane antigen (PSMA) for prostate cancer theranostic application.

Task 5 (Months 9 – 30): In vivo and PET/CT imaging evaluation of the synthesized theranostic agents (Sun)

The therapeutic effect and imaging performance of the theranostic platform are under evaluation in prostate cancer mouse models.

Task 2 (Months 1 – 12): Synthesis & Characterization of CB-TE2A-based Bifunctional Chelator

We performed further work on this Task in the 2nd year of funding.

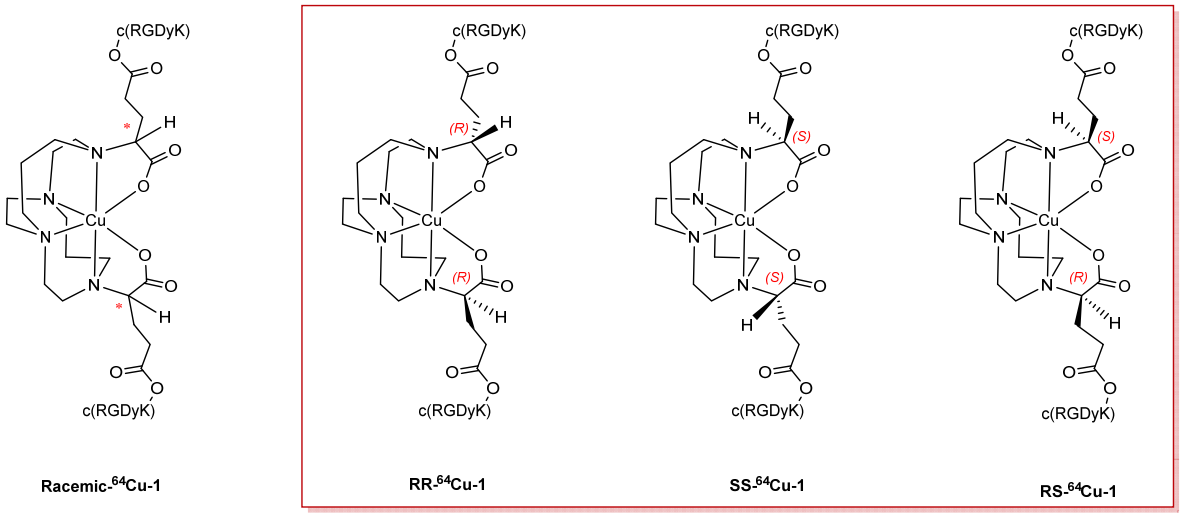

Figure 1. *Structures of peptide conjugates: rac-^{64}Cu-1, RR-^{64}Cu-1, SS-^{64}Cu-1 and RS-^{64}Cu-1.*

It is well recognized that carbon chirality plays a critical role in the design of drug molecules. However, very little information is available regarding the effect of stereoisomerism of macrocyclic bifunctional chelators (BFC) on biological behaviors of the corresponding radiopharmaceuticals. To evaluate such effects, three enantiopure stereoisomers of a copper radiopharmaceutical BFC bearing two chiral carbon atoms were synthesized in forms of R,R-, S,S-, and R,S-. Their corresponding peptide conjugates were prepared by coupling with a model peptide sequence, c(RGDyK), which targets the $\alpha_v\beta_3$ integrin for *in vitro* and *in vivo* evaluation of their biological behaviors as compared to the racemic conjugate. Despite the chirality differences, all the conjugates showed a similar *in vitro* binding affinity profile to the □$_v$□$_3$ integrin (106, 108, 85 and 100 nM for rac-H$_2$-1, RR-H$_2$-1, SS-H$_2$-1, and RS-H$_2$-1 respectively with all p values > 0.05) and a similar level of *in vivo* tumor uptake (2.72 ± 0.45, 2.60 ± 0.52, 2.45 ± 0.48 and 2.88 ± 0.59 for rac-^{64}Cu-1, RR-^{64}Cu-1, SS-^{64}Cu-1, and RS-^{64}Cu-1 at 1 h p.i. respectively). Furthermore, they demonstrated a nearly identical biodistribution pattern in major organs (e.g. 2.07 ± 0.21, 2.13 ± 0.58, 1.70 ± 0.20 and 1.90 ± 0.46 %ID/g at 24 h p.i. in liver for rac-^{64}Cu-1, RR-^{64}Cu-1, SS-^{64}Cu-1, and RS-^{64}Cu-1 respectively; 1.80 ± 0.46, 2.30 ± 1.49, 1.73 ± 0.31 and 2.23 ± 0.71 at 24 h p.i. in kidneys for rac-^{64}Cu-1, RR-^{64}Cu-1, SS-^{64}Cu-1, and RS-^{64}Cu-1 respectively). Therefore we conclude that the chirality of BFC plays a negligible role in $\alpha_v\beta_3$-targeted copper radiopharmaceuticals. However, we believe it is still worthwhile to consider the chirality effects of BFCs on other targeted imaging or therapeutic agents.

1. Results:

1.1. Synthesis:

The synthesis of enantiopure RR-H_2-1, SS-H_2-1, and RS-H_2-1 was achieved in three steps; i) synthesis of the chiral side arms, S-6 and R-6 ii) synthesis of the BFC scaffolds, RR-8, SS-8, and RS-8, and iii) conjugation of two molecules of c(RGDyK) on to the BFCs (Schemes 1 - 3). The synthesis of the chiral side arms, S-6 and R-6, started from L- and D- glutamic acid, respectively. Following a reported procedure[1, 2], L- or D-glutamic acid was converted to S- or R-2 respectively, via diazotization using sodium nitrite ($NaNO_2$) in the presence of excess HCl in 78% yield. The stereoselectivity of the conversion of L- glutamic acid to S-2 depends critically on both the rate of the addition of the aqueous $NaNO_2$ solution to the acidic L-glutamic acid solution and on the reaction temperature that must be maintained between 0-5 °C during the addition[2]. The synthesis of S-2 uses the stereoselectivity of the deamination reaction, which is known to proceed with complete retention of the configuration [1]. The *t*Bu-protected ester S-3 was synthesized in 55% yield using a standard esterification procedure, namely 4-dimethylaminopyridine (DMAP) and *N, N'*-dicyclohexylcarbodiimide (DCC) in tetrahydrofuran (THF). Unlike the reported procedure where S-3 was synthesized from the acid chloride of S-2, the DMAP/DCC directed esterification was easy to handle and the product, lactone S-3, could be purified and obtained at gram scale. The obtained S-3 was then hydrolyzed using one equivalent of 1N KOH to provide the potassium salt of S-4. A small sample of the above synthesized salt was treated with 3N HCl to yield the corresponding acid in 60% yield for purification and characterization purposes. The carboxylate salt of S-4 was alkylated with benzyl bromide (BnBr) in dimethylformamide (DMF) to afford the crude S-5, an orthogonally protected diester. Purification of crude S-5 using column chromatography yielded the pure product in 52% yield. The secondary alcohol of S-5 was then converted to the corresponding mesylate as a leaving group to provide S-6 in quantitative yield. Mesylate was chosen as the leaving group based on the fact that it is stable in aqueous workup at room temperature and the controlled alkylation of CB-cyclam by S_N2 reaction affords the complete inversion of stereochemistry of the product.

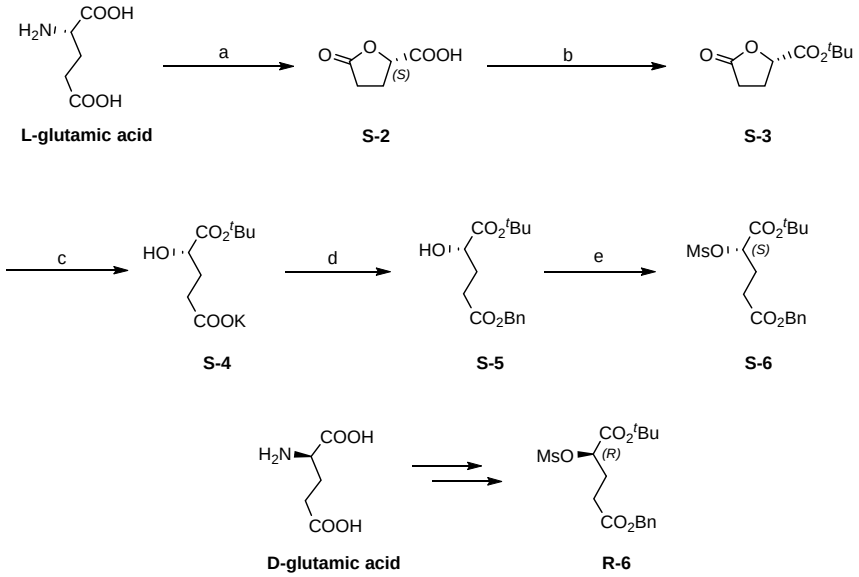

Scheme 1. *Synthesis of 5-benzyl 1-(tert-butyl) 2-((methylsulfonyl)oxy)pentadioate (S-6) and (R-6). Reagents and conditions: a) L-glutamic acid (1 equiv), HCl_{conc}, $NaNO_2$ (1.5 equiv), H_2O/dioxane, 0 °C then r.t., 20 h; b) t-BuOH (1.1 equiv), DMAP (0.4 equiv), DCC (1.1 equiv), CH_2Cl_2, r.t., 18 h; c) 1N KOH (2 equiv), THF, 0 °C then r.t., 4 h; d) BnBr (1 equiv), DMF, r.t. 8 h; e) MsCl (1.01 equiv), Et_3N (1.4 equiv), CH_2Cl_2, 0 °C then r.t., 2 h.*

Dialkylation of CB-cyclam was carried out by adding the mesylated S-6 or R-6, to a suspension of a half equivalent of CB-cyclam in acetonitrile preheated to 50 °C in the presence of potassium carbonate (Scheme 2). The orthogonally protected diester, RR-7 or SS-7, was obtained in 52% yield. Addition of the chiral side arms, S-6 and R-6, provided the BFC scaffolds RR-7 and SS-7, respectively, with the complete inversion of configuration. The BFC scaffold RS-7 was synthesized in two steps: reaction of CB-cylam with S-6, to yield scaffold R-9, followed by alkylation with R-6 to provide RS-7 in 40% yield (Scheme 3).

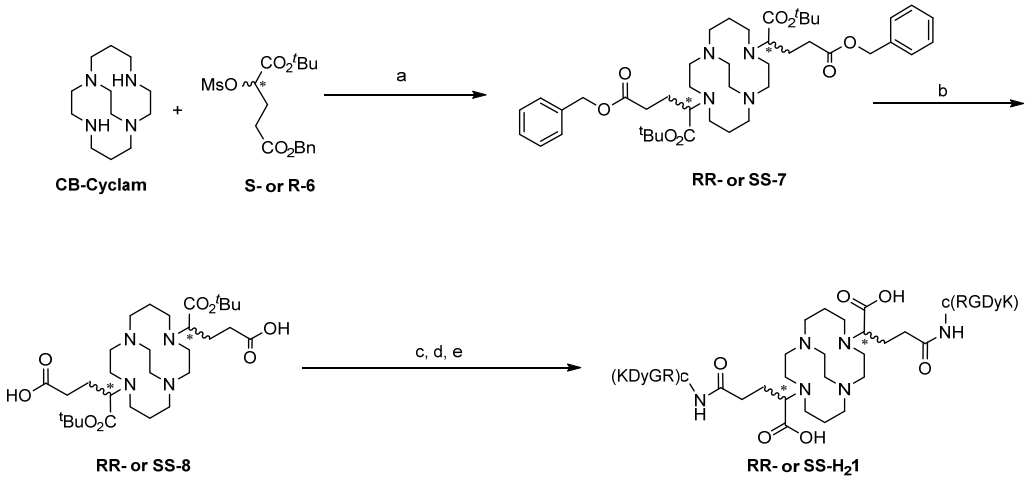

Scheme 2. *Synthesis of RR-H_2-1 and SS-H_2-1. Reagents and conditions: a) K_2CO_3 (1.2 equiv), CH_3CN, r.t. 24 h then 50 °C 24 h; b) 10% Pd/C (catalytic), H_2, 2-propanol, r.t. 12 h; c) NHS (4 equiv), EDC HCl (4 equiv), CH_3CN, r.t. 18 h; d) c(RGDyK) (4 equiv),* DIPEA, DMF, r.t 24 h; e) TFA, r.t. 12 h.

The synthesized BFC scaffolds RR-7, SS-7, and RS-7 contain two protected carboxylate groups at α and γ positions of the side arms. The benzyl protected γ-carboxylate groups were selectively deprotected and the resulting acids were conjugated with the c(RGDyK) peptide. Catalytic debenzylation of RR-7, SS-7, and RS-7 was achieved using 10% Pd/C in 2-propanol under hydrogen atmosphere to afford RR-8, SS-8, and RS-8 in quantitative yield. The obtained γ-carboxylic acids were activated by N-hydroxysuccinimide (NHS) for acid-amine conjugation chemistry. The conjugation of NHS-activated RR-8, SS-8, and RS-8 with two equivalents of c(RGDyK) in the presence of N, N-diisopropylethylamine (DIPEA) provided the *t*-butyl protected conjugates in quantitative yield. Finally, the α-carboxylate groups were deprotected using 95% trifluoroacetic acid to provide RR-H_2-1, SS-H_2-1, and RS-H_2-1, each of which contains two free carboxylic acids for radiolabeling with ^{64}Cu.

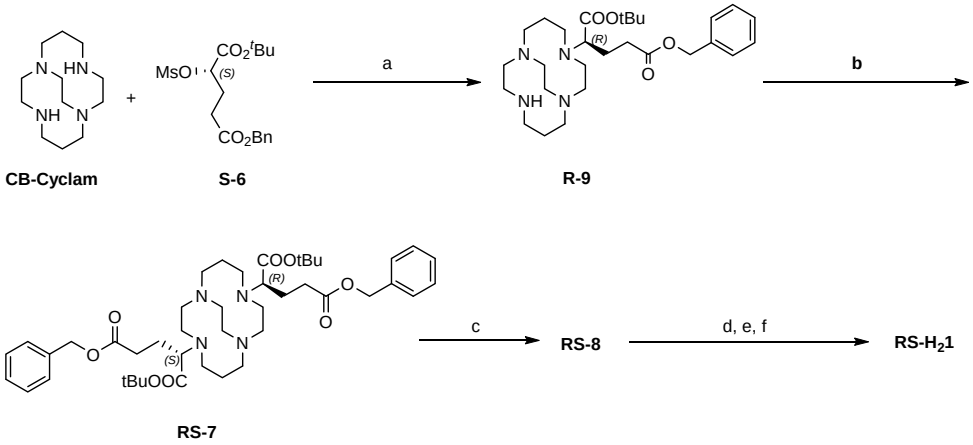

***Scheme 3**. Synthesis of RS-H_2-1. Reagents and conditions: a) K_2CO_3 (1.2 equiv), CH_3CN, r.t. 24 h then 50 °C 24 h; b) R-6 (1.5 equiv), K_2CO_3 (1.2 equiv), CH_3CN, r.t. 24 h then 50 °C 24 h; c) 10% Pd/C (catalytic), H_2, 2-propanol, r.t. 12 h; d) NHS (4 equiv), EDC HCl (4 equiv), CH_3CN, r.t. 18 h; e) c(RGDyK) (4 equiv), DIPEA, DMF, r.t 24 h; f) TFA, r.t. 12 h.*

Compounds, S- or R-2 to S- or R-6 were characterized by ^{1}H and ^{13}C NMR and found to be identical to those reported in the literature [2]. Compounds, S- or R-2 to S- or R-6, showed no differences in ^{1}H and ^{13}C NMR spectra as expected for enantiomers. The peptide conjugates were characterized by their molecular ion peak shown on MALDI-mass spectra, and the purity of the conjugates was verified by HPLC. Optical rotation $[\alpha]_D$ for compounds RR-7 and SS-7 was recorded to be +34.594 and -36.594 respectively, verifying that these compounds are enantiomers. Furthermore, the circular dichroism (CD) spectra measured in CH_3CN:H_2O (1:5) solution, further confirm the enantiomeric nature of the optically active BFC scaffolds, RR-8 and SS-8. The CD spectrum of RR-8 shows a positive Cotton effect in the 230-280 nm region, while SS-8 exhibits the opposite sign of the effect in the same range (Figure 2).

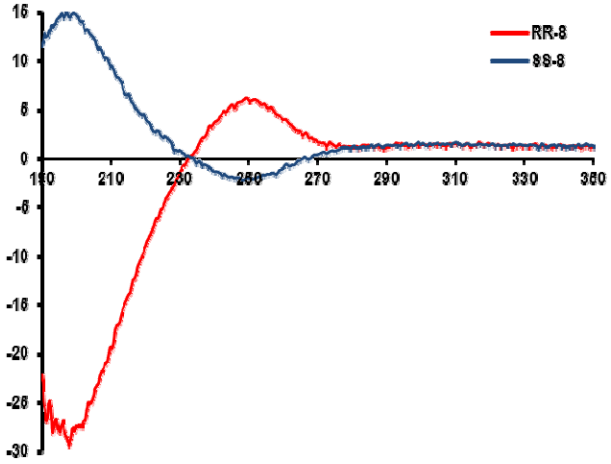

Figure 2. Measured CD spectra of RR-8 and SS-8 in CH_3CN:H_2O 1:5.

1.2. Radiochemistry:

All peptide conjugates (rac-H_2-1, RR-H_2-1, SS-H_2-1, and RS-H_2-1) were successfully labeled (> 90% RCY) with ^{64}Cu within 30 min at 75 °C in 0.4 mM NH_4OAc buffer to provide rac-^{64}Cu-1, RR-^{64}Cu-1, SS-^{64}Cu-1, and RS-^{64}Cu-1, respectively. A series of radiolabeling conditions by decreasing the amount of peptide conjugates while the radioactivity of ^{64}Cu was fixed were tested to reach around 20 GBq/mmol specific activity. The ^{64}Cu-labeled conjugates were purified in one step using a pre-conditioned C-18 Sep-Pak light cartridge with a >90% recovery rate. The radiochemical purity of the ^{64}Cu-labeled conjugates after cartridge purification was >97% as determined by radio-HPLC. The overall radiochemical procedure including the synthesis and purification steps took less than 45 min.

1.3. Binding Assay:

The $\alpha_v\beta_3$ binding affinities of rac-H_2-1, RR-H_2-1, SS-H_2-1, and RS-H_2-1 were measured by a competitive cell-binding assay using U87MG cells in which ^{125}I-echistatin was employed as $\alpha_v\beta_3$-specific radioligand for competitive displacement. The U87MG cell line was chosen because the $\alpha_v\beta_3$ integrin density on the cell surface is the highest among the solid tumor cell lines that have been assessed [3]. The IC_{50} values of rac-H_2-1, RR-H_2-1, SS-H_2-1, and RS-H_2-1 which represent their concentrations required to displace 50% of the ^{125}I-echistation bound on the U87MG cells, were determined to be 106, 108, 85 and 100 nM, respectively (n = 4) with all p values >0.05.

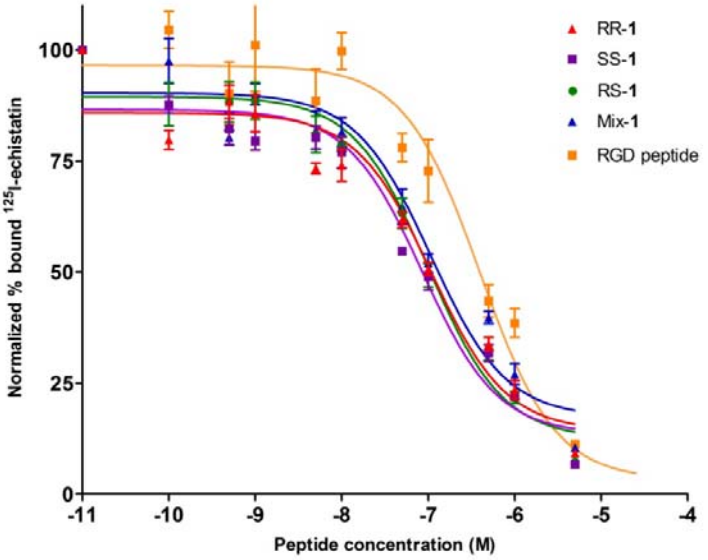

Figure 3. The integrin $\alpha_v\beta_3$ binding affinities of cRGDyK peptide, RR-1, SS-1, RS-1 and rac-1 measured by a competitive cell-binding assay using ^{125}I-echistatin as the radioligand. The IC_{50} values were calculated to be 396 nM (cRGDyK), 108 nM (RR-1), 85 nM (SS-1), 100 nM (RS-1) and 106 nM (rac-1) (R^2: 0.91 – 0.94).

1.4. Small Animal PET-CT Imaging:

To evaluate the effect of the chirality of BFC on the *in vivo* properties of the $\alpha_v\beta_3$-targeted imaging agents, a comparative PET/CT imaging study was performed in SCID mice bearing integrin $\alpha_v\beta_3$-positive PC-3 prostate cancer xenografts on a Siemens Inveon PET/CT Multimodality System. Representative trans-axial PET/CT images at 1, 4, and 24 h p.i. are displayed in Figure 4. The PC-3 tumors were clearly visualized by all four probes up to 24 h p.i. The four agents showed nearly identical tumor uptake at the three time points, namely 2.72 ± 0.45, 2.60 ± 0.52, 2.45 ± 0.48 and 2.88 ± 0.59 for rac-^{64}Cu-1, RR-^{64}Cu-1, SS-^{64}Cu-1, and RS-^{64}Cu-1 respectively at 1 h p.i., 2.32 ± 0.37, 2.13 ± 0.49, 1.58 ± 0.32 and 1.73 ± 0.36 at 4 h p.i and 1.77 ± 0.32, 1.92 ± 0.51, 1.16 ± 0.20 and 1.22 ± 0.31 at 24 h p.i. with all p values > 0.05 except for SS-^{64}Cu-1 that showed significantly lower uptake than other conjugates at 4 and 24 h p.i. due to its lower specific activity at the injection time. In addition, we compared their *in vivo* distribution profiles in major organs and found that the stereoisomers shared a similar biodistribution pattern in the mouse tumor model.

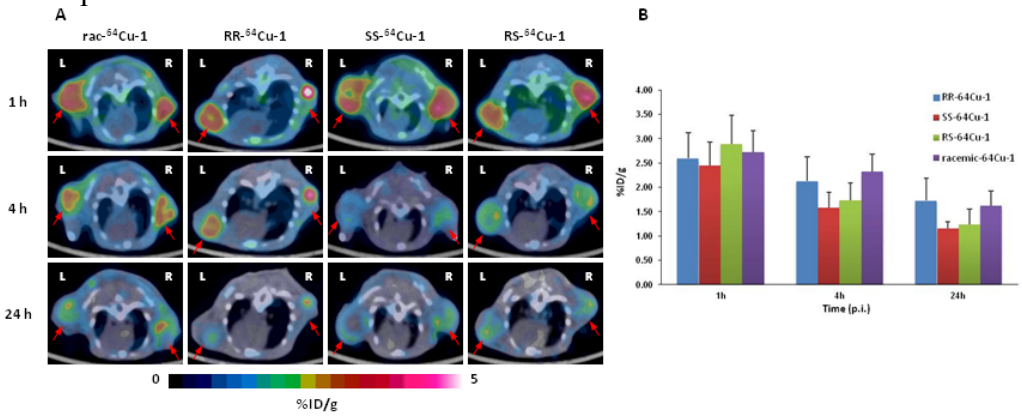

Figure 4*: (A) Comparative transaxial PET/CT images of PC-3 tumors in SCID mice intravenously injected with rac-^{64}Cu-1, RR-^{64}Cu-1 , SS-^{64}Cu-1 , and RS-^{64}Cu-1 at 1 h, 4 h, and 24 h p.i. (B) Quantitative tumor uptake analysis of the four ^{64}Cu-labled peptide conjugates (n = 6).*

2. Experimental Section

2.1. General Methods and Materials.

All reactions were carried out under N_2 atmosphere in degassed dried solvents. Commercially available starting materials were purchased from vendors and used directly without further purification unless otherwise stated. Milli-Q water (18 MΩ·cm) was obtained from a Millipore Gradient Milli-Q water system (Billerica, MA). All aqueous solutions were prepared with Milli-Q water. Silica gel 60 (70-230 mesh, Merck) was used for column chromatography. Analytical thin-layer chromatography (TLC) was performed using F254 silica gel (precoated sheets, 0.2 mm thick) (Lawrence, KS). ^{1}H and ^{13}C NMR spectra were recorded on a Varian 400 spectrometer; chemical shifts are expressed in ppm relative to TMS (0.0 ppm). Matrix-assisted laser desorption/ionization (MALDI) mass spectra were acquired on an Applied Biosystems Voyager-6115 mass spectrometer. Optical rotation data were collected on a APIV-6W Rudolph Research automatic polarimeter. Radiolabeled conjugates were purified by Light C-18 Sep-Pak cartridges (Waters, Milford, MA).

Bulk solvents were removed by rotary evaporator under reduced pressure, and trace solvents were removed by vacuum pump. 1,4,8,11-tetraazabicyclo[6.6.2]hexadecane (CB-cyclam) was synthesized according to a published procedure[4]. $^{64}Cu(II)$ in 0.1M HCl was purchased from either Washington University School of Medicine in St. Louis or the University of Wisconsin at Madison.

2.2. High Performance Liquid Chromatography (HPLC) Methods. HPLC separation was performed on a Waters 600 Multisolvent Delivery System equipped with a Waters 2996 Photodiode Array detector. The mobile phase consisted of H_2O with 0.1% TFA (solvent A) and acetonitrile with 0.1% TFA (solvent B). The analytical HPLC was performed on an XTerra RP18 column (150 × 4.6 mm) with a gradient of 0% B to 100% B in 50 min at the flow rate of 1.0 mL/min. The HPLC separation was performed on a semi-preparative XTerra RP18 Column (250 × 10 mm) with a gradient of 0% B to 100% B in 50 min at the flow rate of 4.0 mL/min.

2.3. Integrin $\alpha_v\beta_3$ Binding Assay. The binding affinities of c(RGDyK), rac- H_2-1, RR-H_2-1, RS-H_2-1, and SS-H_2-1 to integrin $\alpha_v\beta_3$ were determined by a competitive cell-binding assay using ^{125}I-echistatin (PerkinElmer) as the $\alpha_v\beta_3$-specific radioligand. The experiments were performed on U87MG human glioblastoma cells following our previously reported method[5]. Briefly, U87MG cells were grown in RPMI 1640 medium supplemented with penicillin, streptomycin, and 10% (v/v) fetal bovine serum (FBS) at 37 ºC under 5% CO_2. Suspended U87MG cells in binding buffer (20 mM Tris, pH 7.4, 150 mM NaCl, 2 mM $CaCl_2$, 1 mM $MgCl_2$, 1 mM $MnCl_2$, 0.1% bovine serum albumin) were seeded on multi-well DV plates (Millipore) with 5×10^4 cells per well and then incubated with ^{125}I-echistatin (10,000 cpm/well) in the presence of increasing concentrations (0 – 5,000 nM) of c(RGDyK) peptide conjugates for 2 h. The final volume in each well was maintained at 250 μL. At the end of incubation, unbound ^{125}I-echistatin was removed by filtration followed by five rinses with cold binding buffer. The retentive was collected and the radioactivity was measured using a γ-counter. The best-fit IC_{50} values (inhibitory concentration where 50% of the ^{125}I-echistatin bound on U87MG cells are displaced) of c(RGDyK), rac-H_2-1, RR-H_2-1, SS-H_2-1, and RS-H_2-1were calculated by fitting the data with nonlinear regression using GraphPad Prism (GraphPadSoftware, Inc.). Experiments were duplicated with quintuplicate samples.

2.4. Tissue Culture and Animal Model. All animal studies were performed in compliance with guidelines set by the UT Southwestern Institutional Animal Care and Use Committee (IACUC). The PC-3 cell line was obtained from the American Type Culture Collection (ATCC,

Manassas, VA), and was cultured in T-media (Invitrogen, Carlsbad, CA) at 37 °C in an atmosphere of 5% CO_2 and were passaged at 75% confluence in P150 plates. T-media was supplemented with 5% Fetal Bovine Serum (FBS) and 1 × Penicillin/Streptomycin. PC-3 cells were harvested from monolayer using PBS and trypsin/EDTA, and suspended in T-media with 5% FBS. The cell suspension was then injected subcutaneously (5×10^5 cells in 100 μL media) into the front flanks of male SCID (Severe combined immunodeficiency) mice. After injection, animals were monitored three times a week by general observations. The tumor was allowed to grow three weeks to reach a palpable size (50-150 mm^3) for microPET/CT imaging studies.

2.5. Mouse PET/CT Imaging. The imaging studies were performed on a Siemens Inveon Multimodality PET/CT system once the tumor size reached the range of 50-150 mm^3 (tumor volume = ½(length × $width^2$). One hour prior to imaging, each mouse bearing PC-3 tumor was injected with 100 – 125 μCi of a ^{64}Cu labeled conjugate in 100 μL of saline *via* the tail vein. Ten minutes prior to imaging, the animals were anesthetized using 3% isofluorane at room temperature until stable vitals were established. Once the animal was sedated, it was placed onto the imaging bed under 2% isofluorane anesthesia for the duration of imaging data requisition. At each time point (1 h, 4 h, and 24 h) post-injection (p.i.), a CT scan was performed (8 min), followed immediately by a static PET scan (15 min). The CT imaging was acquired at 80 kV and 500 μA with a focal spot of 58 μm. The total rotation of the gantry was 360^o with 360 rotation steps obtained at an exposure time of approximately 180 ms/frame. The images were attained using CCD readout of 4096 × 3098 with a binning factor of four and an average frame of one. Under low magnification the effective pixel size was 103.03 μm. The CT images were reconstructed with a down sample factor of two using Cobra Reconstruction Software. PET images were reconstructed using Fourier Rebinning and Ordered Subsets Expectation Maximization 3D (OSEM3D) algorithm. Reconstructed CT and PET images were fused and analyzed using the manufacturer's software. For quantification, regions of interest were placed in the areas expressing the highest ^{64}Cu-labeled conjugate activity as determined by PET and visually guided by CT images. The tissues examined include the tumor, heart, liver, lung, kidney, and muscle. The resulting quantitative data were expressed in percentage of the injected dose in per gram of the tissue (%ID/g) on the assumption that the density of the tissue is 1 g/cm^3.

2.6. Synthesis:

2.6.1. Synthesis of (*S*)-5-oxotetrahydrofuran-2-carboxylic acid (S-2). L-glutamic acid (30.0 g, 200 mmol) was suspended in a water/dioxane mixture (75/25 mL) and stirred at 0 °C for 30 min. The white slurry became clear after 40 mL of concentrated HCl (37%) was added, followed by drop-wise addition of a solution of $NaNO_2$ (21.0 g, 300 mmol) in 50 mL of water. The reaction temperature was maintained around 0 °C during the 4 h of addition. The reaction mixture was then left stirring at room temperature for 20 h. Upon completion, the solvent was evaporated under reduced pressure to provide a white solid, which was then treated with EtOAc (300 mL) and Na_2SO_4 for 30 min. The solution was filtered and the solvent was evaporated to yield S-2 as a white solid (21.50 g, 78%). ^{1}H NMR (400 MHz, $CDCl_3$) δ 11.08 (bs, 1H), 5.01 (m, 1H), 2.71-2.55 (m, 3H), 2.45-2.37 (m, 1H); ^{13}C NMR (100 MHz, $CDCl_3$) δ 176.8, 174.5, 75.4, 26.8, 25.7.

2.6.2. Synthesis of *tert*-butyl (*S*)-5-oxotetrahydrofuran-2-carboxylate (S-3). In a solution of S-2 (10.0 g, 77 mmol) in CH_2Cl_2 (240 mL), *t*-butanol (8 ml, 84 mmol) and 4-dimethylaminopyridine (DMAP, 3.75 g, 31 mmol) were added and the reaction mixture was cooled to 0 °C. To this solution, N, N-dicyclohexylcarbodiimide (DCC, 16.2 g, 84.5 mmol) in CH_2Cl_2 (80mL) was added dropwise. The reaction was stirred at room temperature overnight and upon completion the solvent was removed under reduced pressure. The residue was purified by column chromatography (silica gel, gravity) using hexane (250 mL) and EtOAc:hexane (1:4) to

give S-3 as white solid (7.0 g, 55%) : ^{1}H NMR (400 MHz, $CDCl_3$) δ 4.79 (m, 1H), 2.65-2.44 (m, 3H), 2.24 (m, 1H), 1.48 (s, 9H) ppm; ^{13}C NMR (100 MHz, $CDCl_3$) δ 176.2, 169.0, 83.1, 76.2, 27.9, 26.8, 25.8 ppm.

2.6.3. Synthesis of potassium (*S*)-5-(*tert*-butoxy)-4-hydroxy-5-oxopentanoate (S-4). Compound S-3 (5.0 g, 30 mmol) was dissolved in THF (60 mL), and cooled to 0 °C. To this mixture, 1N KOH (aqueous, 66 mL) was added dropwise. The resulting mixture was stirred at room temperature over 4 h and upon completion the solvent was evaporated to give S-4 as white solid. Compound S-4 was directly used for the synthesis of S-5. However, for characterization of the compound, a sample of S-4 was converted to its acid using 3N hydrochloric acid. The acidified aqueous layer was then extracted with EtOAc (3 × 30 mL). The organic layers were combined and dried over anhydrous $MgSO_4$ and concentrated. The residue was purified by column chromatography (silica gel, gravity) using hexane (100 mL) and EtOAc:hexane (1:3) to yield the acid form of S-4 as a white solid (3.0 g, 60%) : ^{1}H NMR (400 MHz, $CDCl_3$) δ 4.10 (m, 1H), 2.57-2.41 (m, 2H), 2.16-2.07 (m, 1H), 1.92-1.83 (m, 1H), 1.47 (s, 9H); ^{13}C NMR (100 MHz, $CDCl_3$) δ 178.6, 173.9, 82.8, 69.5, 29.4, 29.0, 27.8.

2.6.4. Synthesis of 5-benzyl 1-(*tert*-butyl) (*S*)-2-hydroxypentanedioate (S-5). S-4 (2.0 g, 9.8 mmol) was suspended in DMF (15 mL), to which was added benzyl bromide (1.67 g, 9.8 mmol). After stirred for 8 h, the mixture was poured into ice water (20 mL) and extracted with EtOAc (3 × 25 mL). The combined organic layer was dried over Na_2SO_4 and concentrated under reduced pressure. The residue was purified by column chromatography (silica gel, gravity) using hexane and EtOAc:hexanes (1:4) to give S-5 as a white solid (1.5 g, 52%) . ^{1}H NMR (400 MHz, $CDCl_3$) *δ* 7.35 (m, 5 H), 5.13 (s, 2 H), 4.08 (bs, 1 H), 2.88 (bs, 1 H), 2.59-2.44 (m, 2 H),2.17 (m, 2 H), 1.91 (m, 1 H), 1.48 (s, 9 H). ^{13}C NMR (100 MHz, $CDCl_3$) *δ* 173.9, 173.0, 135.9, 128.5, 128.2, 128.1, 82.8, 69.6, 66.3, 29.7, 29.4, 28.0.

2.6.5. Synthesis of 5-benzyl 1-(*tert*-butyl) (*S*)-2-((methylsulfonyl)oxy)pentadioate (S-6). Methanesulfonyl chloride (0.42 g, 3.7 mmol) was added to a mixture of S-5 (1.0 g, 3.4 m mol) and Et_3N (0.47 g, 4.7 mmol) in CH_2Cl_2 (25 mL) at 0-5 °C. After the addition was completed, the mixture was warmed to room temperature and stirred for 2 h. Upon completion, water (10 mL) was added, the organic phase was separated and washed with brine (3 × 10 mL), dried over Na_2SO_4 and concentrated to give S-6 (0.7 g, 60%). ^{1}H NMR (400 MHz, $CDCl_3$) *δ* 7.36 (m, 5 H), 5.14 (s, 2 H), 4.98 (m, 1 H), 3.11 (s, 3 H), 2.55 (m, 2 H), 2.30 (m, 1 H), 1.49 (s, 9 H). ^{13}C NMR (100 MHz, $CDCl_3$) *δ* 171.8, 167.4, 135.5, 128.5, 128.2, 128.2, 83.5, 76.6, 66.5, 38.9, 29.3, 27.8, 27.0.

The synthesis of 5-benzyl 1-(*tert*-butyl) (*R*)-2-((methylsulfonyl)oxy)pentadioate (R-6) was accomplished in the same way as above from D-glutamic acid.

2.6.6. Synthesis of compound RR-7: Compound S-6 (500 mg, 1.3 mmol) was added to a suspension of cross-bridge cyclam (150 mg, 0.6 mmol) and K_2CO_3 (0.10 g) in anhydrous acetonitrile (50 mL). The reaction was stirred at room temperature for 24 h and then for another 24 h at 50 °C. The reaction mixture was filtered and the solid was washed twice with chloroform (2 × 20 mL). The combined filtrates were concentrated under reduced pressure and purified by column chromatography (silica gel, 60-230 mesh) using 10:1 $CHCl_3$/MeOH to 9:1 EtOAc/isopropylamine to yield RR-7 as viscous oil (250 mg; Yield: 52%): MALDI-TOF/MS [M^+]: calc':778.49; found:778.59

2.6.7. Synthesis of compound RR-$H_2$1. To a solution of RR-7 (13 mg, 16.7 □mol) in 0.5 mL of 2-propanol was added portion wise 10 mg of 10% Pd/C. The suspension was shaken in a hydrogenator (Parr, Moline, Illionis) at room temperature for 12 h under an H_2 atmosphere (60 psi). After removal of the solids, evaporation of the solvent afforded compound RR-8 as a white foam in nearly quantitative yield. A mixture of compound RR-8 (10.0 mg, 16.7 μmol), *N*-hydroxysuccinimide (7.6 mg, 66.8 μmol) and EDC·HCl (12.8 mg, 66.8 μmol) in 500 μL of dry acetonitrile (MeCN) was stirred under N_2 for overnight. The solvent was removed under reduced pressure and the residue was redissolved in $CHCl_3$ (1 mL) and then washed with water promptly three times (3 × 2 mL). $CHCl_3$ was evaporated under reduced pressure, the residue was frozen by liquid nitrogen and the remaining water was removed by a freeze dryer to give a pale yellow solid in quantitative yield. The activated ester was used directly for the next reaction without further purification. Cyclic Arg-Gly-Asp-D-Tyr-Lys [c(RGDyK)] (10 mg, 16 μmol) was mixed with the activated ester (2.4 mg, 4 μmol) in 200 μL of anhydrous DMF. To this solution, 30 μL of N, N-diisopropylethylamine (DIPEA) were added. The mixture was stirred at room temperature for 24 h under N_2. Upon completion, the solvent was evaporated under reduced pressure and the crude product was purified by HPLC. The collected fractions were combined and lyophilized to yield the *t*-butyl protected product, which was then dissolved in 95% TFA and stirred at room temperature for 12 h. After evaporation of the solvent, the residue was purified by semi-preparative reverse-phase HPLC. The collected fractions from multiple runs were collected and lyophilized to afford RR-$H_2$1 as white solid at quantitative yield. MALDI-TOF/MS [M+H^+]: calc'd: 1689.87; found: 1690.67

2.6.8. Synthesis of compound SS-$H_2$1: Compound SS-$H_2$1 was synthesized in a similar manner starting from CB-Cyclam and R-6. MALDI-TOF/MS [M+H^+]: calc'd: 1689.87; found: 1690.67

2.7. Radiolabeling of rac- H_2-1, RR-H_2-1, RS-H_2-1, and SS-H_2-1 with ^{64}Cu. To a 1.5 mL vial containing 5 μg of respective conjugate in 200 μL of 0.4 M NH_4OAc (pH = 6.5) solution, 2-3 mCi of ^{64}Cu(II) in 0.1 M HCl were added. The reaction mixture was shaken and incubated at 75 ºC for 0.5 h. Then, 5 μL of 5 mM diethylenetriaminepentaacetic acid (DTPA) was added into the reaction mixture and allowed to incubate for another 5 min. After incubation, purification of ^{64}Cu-labeled conjugate was carried out by passing the mixture through a preconditioned Sep-Pak C-18 light cartridge. After thorough rinsing (3 × 3 mL water) of the cartridge, the ^{64}Cu-labeled conjugate was eluted by an ethanol-water mixture (70:30). Radio-TLC analysis was performed on a Rita Star Radioisotope TLC Analyzer (Straubenhardt, Germany) to monitor the radiolabeling efficiency via ITLC paper, developed by 10 mM PBS. High performance liquid chromatography (HPLC) analysis was conducted to determine radiochemical purity of the products on a Waters 600 Multisolvent Delivery System equipped with a Waters 2996 Photodiode Array (PDA) detector and an in-line Shell Jr. 2000 radio-detector (Fredericksburg, VA) on a Waters Xtera column (150×4.6 mm, 5 μm). The gradient mobile phase started with 100% A (0.1% TFA in H_2O) to 50% B (0.1% TFA in MeCN) and 50% A at 25 min with a flow rate of 1 mL/min.

2.8. Statistical Analysis. Quantitative data were expressed as the mean ± SD. Unpaired *t* test (two-tailed, confidence intervals: 95%) was performed using GraphPad Prism. *P* values of < 0.05 were considered statistically significant.

Task 4 (Months 13 – 24): Synthetic and radio- chemistry and in vitro assay of the synthesized theranostic agents (Sun/Hsieh)

Targeted therapy has become attractive approaches to extend the therapeutic window. In contrast with antibody drug conjugates (ADCs), molecular drug conjugates (MDCs) possess superior

properties like faster pharmacokinetics, better solid tumor penetration, and lower manufacturing cost. Integration of non-invasive imaging has demonstrated critical importance for targeted therapy. The recently reported *all-in-one* approach permits concurrent monitoring and treatment, while still leaving a gap between preclinical and clinical if via optical imaging. Therefore, we propose to develop MDCs integrated with PET imaging functionality, and hypothesize it can promote the personalized prostate cancer treatment by combining imaging and therapy.

1. Results

1.1. Organic chemistry

According to the overall design of MDCs, we separate the entire synthesis into several subunits as shown in **Scheme 1**. The PSMA targeting ligand ***4*** has been synthesized in a conventional chemistry way [6]. To retain the PSMA targeting ligand affinity after integration into the MDCs, a PEG_5 and a Boc-lysine linker has been introduced to form compound ***5***, as well as an aldehyde unit. Then, the fluorine component ***3*** and ligand ***5*** were reacted together, followed by a two-step coupling reactions with the most expensive DM1 drug payloads. The disulfide exchange will form *[^{19}F]**9a*** to enable the drug releasing inside cancer cells, while maleimide covalent formation of [^{19}F]***9b*** will be used for comparison. To obtain the paired [^{18}F]***9a,b***, the synthetic route will be slightly different, since we need to have a primary amine group available for ^{18}F-SFB conjugation. Compounds ***1–7 and 4'*** have been successfully synthesized and characterized by Mass spectra.

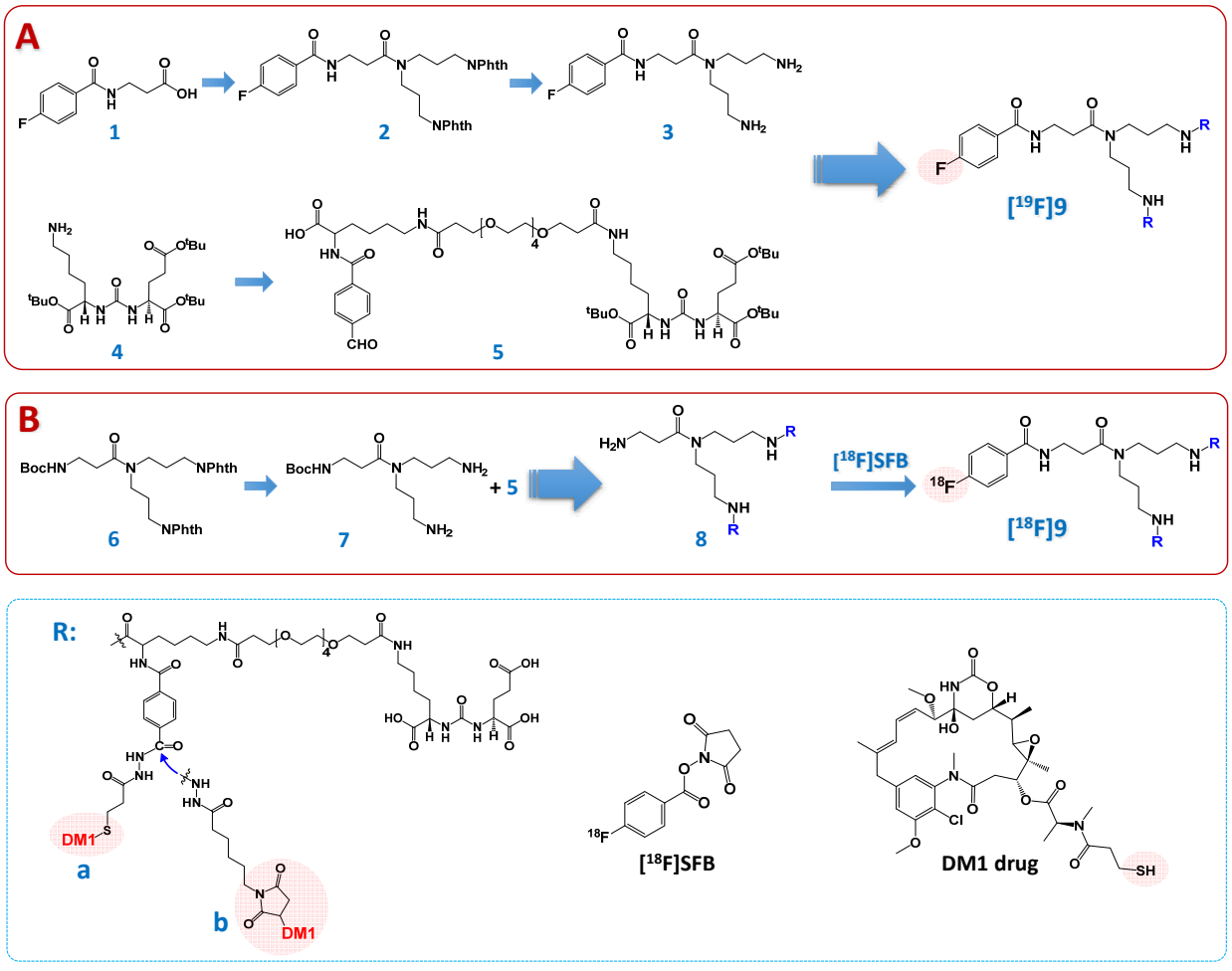

***Scheme 1**. Synthesis route for the [$^{18/19}$F]-dimer (**9**) and [$^{18/19}$F]-monomer (**10**). (**A**) The fluorine component started from ligand **1** and extended to get ligand **2**. After deprotection, ligand **3** has two available amine groups to form a dimer. The lysine-glutamate urea based PSMA targeting ligand **4** was prepared in a large amount according to ref [6]. A PEG$_5$ linker and a Boc-Lysine were used to couple ligand **4** to acquire the intermediate **5**. The final [^{19}F]**9** can be led by the coupling between the fluorine component and the targeting ligand, followed by the therapeutic payload (DM1) conjugation either by disulfide exchange [^{19}F]**9a** or maleimide covalent bonding [^{19}F]**9b**. (**B**) The corresponding [^{18}F]**9a,b** can be prepared from **6** to **8** in a similar route with [^{19}F]**9**, and then get labeled with ^{18}F-SFB via the only available primary amine group in ligand **8**.*

1.2. Radiochemistry

According to a recently improved procedure [7, 8], we have successfully established our own protocol to routinely acquire ^{18}F-SFB in a 45-min period (**Scheme 2**). This radiolabeling improvement can significantly save the time to prepare [^{18}F]MDCs, which allows us to spend more efforts on imaging and therapy evaluations.

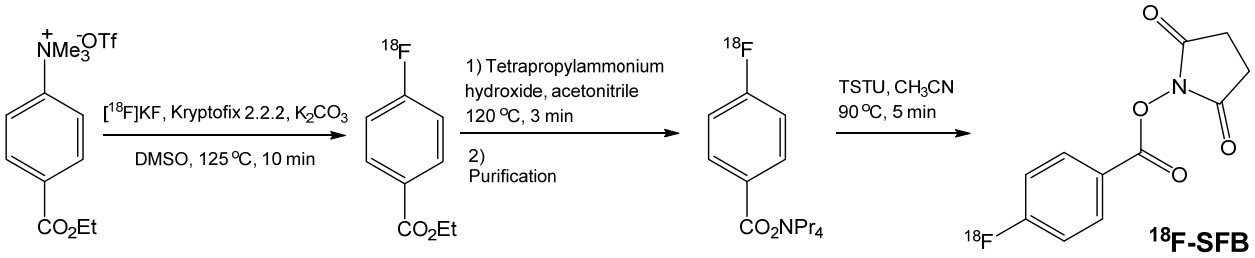

***Scheme 2**. Radiolabeling procedure for ^{18}F-SFB with the TRACERlab FX N synthesizer.*

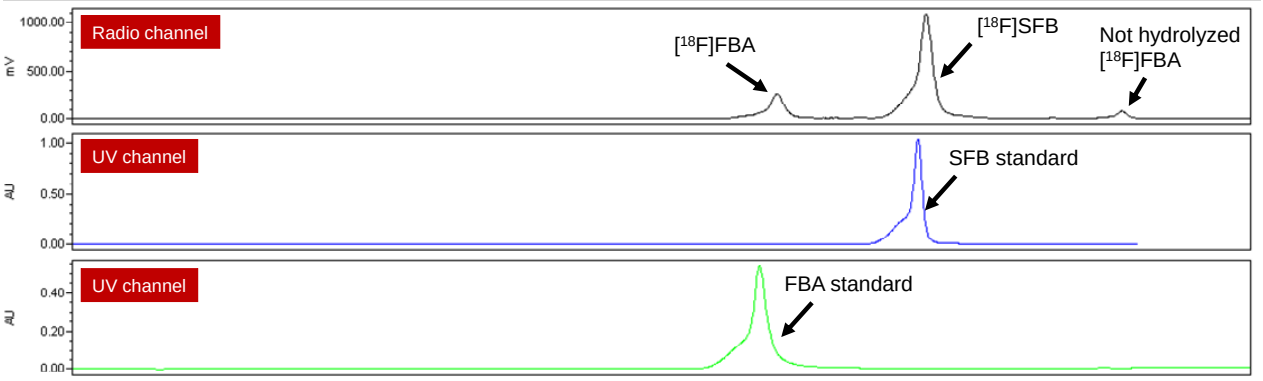

Figure 2. HPLC characterization of ^{18}F-SFB and the intermediate ^{18}F-FBA. HPLC conditions: A: 0.1%TFA, H_2O; B: 0.1%TFA, Acetonitrile; Gradient: 0-30 min, 0-60% B; 1 mL/min

2. Methods

2.1. Organic synthesis

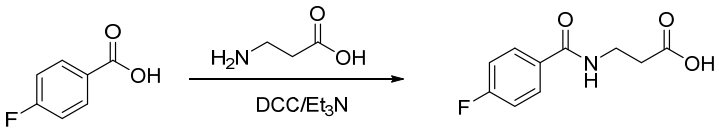

3-(4-fluorobenzamido)propanoic acid (1) To a solution of 4-fluorobenzoic acid (0.30 g, 2.14 mmol) in DMF (3.0 mL) was added β-alanine (0.25 g, 2.78 mmol) and triethyl amine (0.28 g, 2.78 mmol) and the suspension was stirred overnight. The resulting solution was filtered and the solvent was evaporated under reduced pressure. The resulting crude mixture was purified using flash chromatography with silica as stationary phase and ethyl acetate as mobile phase. (Yield: 35%). MS (ESI) *m/z* calcd for $C_{10}H_{10}FNO_3$: 211.0; found: 211.9 ($[M + H]^+$).

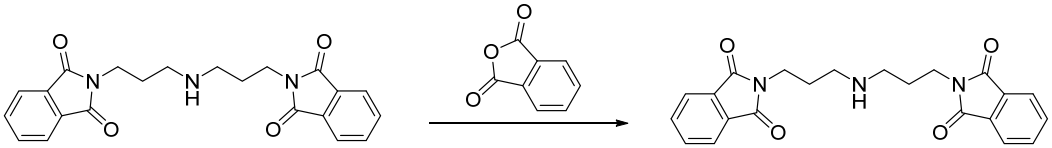

2,2'-(azanediylbis(propane-3,1-diyl))bis(isoindoline-1,3-dione). Bis(phthalimidylpropyl)amine (**2**) was synthesized following a previously published report.[9] Briefly, phthalic anhydride (5.0 g, 33.8 mmol) was added to a solution of bis(3-aminopropyl)amine (2.03 g, 15.5 mmol) in toluene/DMF (50 mL/5 mL). The reaction mixture was stirred under reflux for 24 hours. The solvent was then evaporated and EtOH (100 mL) added to the residue. The resultant mixture was stirred for 5 hours, and the precipitate filtered, and dried to give the compound **2.** (Yield: 45%) ^{1}H NMR (400 MHz, $CDCl_3$): δ = 7.83 (m, 4H), 7.70 (m, 4H), 3.75 (t, J = 6.8 Hz, 4H), 2.62 (t, J = 6.8 Hz, 4H), 1.84 (quintet, J = 6.8 Hz, 4H).

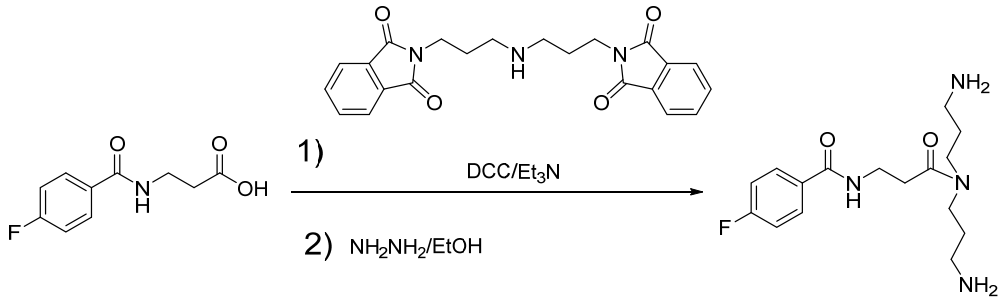

N-(3-(bis(3-aminopropyl)amino)-3-oxopropyl)-4-fluorobenzamide (3) To a solution of acid **1** (0.3 g, 1.41 mmol) in ACN (3.0 mL) was added the secondary amine, **2** (0.66 g, 1.69 mmol), dicyclohexylcarbodiimide (0.29 g, 1.41 mmol) and triethylamine (0.17 g, 1.69 mmol). The resultant solution was stirred for 12 hours, filtered and the solvent evaporated. The crude product was purified by flash chromatography (ethyl acetate). (Yield: 43%). The resultant compound was dissolved in ethanol (5 mL) and hydrazine monohydrate (0.1 mL, 2.0 mM) was added. The mixture was stirred for 12 h at room temperature. After the reaction, the precipitate was removed by filtration. The filtrate was evaporated and extracted with CH_2Cl_2 (3 x 10 mL). The combined organic layers were evaporated to give light yellow oil **3** MS (ESI) *m/z* calcd for $C_{16}H_{25}FN_4O_2$: 324.2; found: 325.6 ($[M + H]^+$).

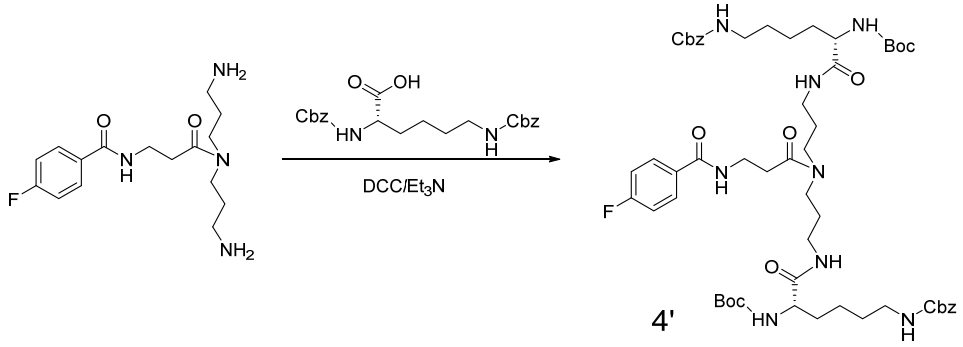

Compound 4' To a solution of diamine **3** (0.1 g, 0.31 mmol) in ACN (3.0 mL) was added the secondary protected lysine (0.13 g, 0.31 mmol), dicyclohexylcarbodiimide (0.06 g, 0.31 mmol)

and triethylamine (0.03 g, 0.31 mmol). The resultant solution was stirred for 12 hours, filtered and the solvent evaporated. The crude product was purified by flash chromatography (ethyl acetate). MS (ESI) *m*/*z* calcd for $C_{54}H_{77}FN_8O_{12}$: 1048.6; found: 1049.0 ($[M + H]^+$).

2.2. Radiolabeling of ^{18}F-SFB

The $[^{18}F]F^-$, produced via $^{18}O[p,n]^{18}F$ nuclear reaction, is separated from remaining $[^{18}O]H_2O$ using an anion exchange column (QMA cartridge, Waters).The $^{18}F^-$-ions are adsorbed on the ion exchange resin while the passing $[^{18}O]H_2O$ is recovered. A mixture of 0.4 mL of K_{222}/K_2CO_3 solution (3.0 mg K_2CO_3 and 15 mg K_{222}) and 1 mL of ACN is used for elution of the adsorbed fluoride.

Drying is executed by azeotropic distillation of the water with acetonitrile. To eliminate all water traces, the drying takes place in two steps (60°C with inert gas and 100°C at vacuum) and dry with another 1 mL acetonitrile one more time. It is dried one more time by additional 1 mL of ACN. To evaporate and dry the solution quantitatively is essential as OH--anions caused by water dissociation compete with the F^--anion during reaction and can reduce the $[^{18}F]$-labeling yield considerably. In this step 5.3 mg of the precursor (trimethylbenzeneaminium triflate) dissolved in 0.5 mL of DMSO is added to the reaction vessel. The solution is heated for 10 minutes at 125 °C in the sealed reactor. The intramolecular leaving group is substituted by $^{18}F^-$ under the presence of K_{222}.

After this time, tetrapropylammonium hydroxide (TPAH, 20 µl in 0.5 ml of MeCN) was added to saponify the ester group. Heating at 120°C for 3 min provided $[^{18}F]$4-fluorobenzoic acid ($[^{18}F]$FBA) as the corresponding TPA salt. After saponification, 1 ml of acetonitrile was added and evaporated (70°C, 5 min) with a stream of argon to remove any residual water left over from the saponification.

O-(N-succinimidyl)-1,1,3,3-tetramethyluronium tetrafluoroborate (TSTU, 10 mg in 0.6 ml of MeCN) was added and the reaction vessel was heated at 90°C for 5 min to provide $[^{18}F]$SFB. The crude reaction mixture was cooled down (40°C) and transferred to the dilution flask (pre-charged with 20 ml of 1.5 % acetic acid solution). The resulting solution was transferred through a Waters C18 Plus Long sep-pak and the C18 sep-pak was then washed with 10% MeCN (10 ml). Following washing, elution into the collection vial with neat MeCN (2 ml) gave ^{18}F-SFB mixture (87 mCi). 10 mCi remained in the C18 cartridge. The ^{18}F-SFB could be used as the obtained solution in MeCN or, alternatively, could be evaporated to dryness (heat gun) and re-dissolved in DMSO.

2.3. Cell membrane protein extraction

LNCaP cells were cultured in RPMI1640 media under 5% CO_2 at 37°C. The media was changed to PBS free media and incubated for 24 h. Decant growth media from cell surface. 2. Wash cell surface with ice-cold HEPES-buffered saline. Add ~5 ml of ice-cold HEPES-buffered saline to cells and loosen cells from the surface with a cell scraper. Place the cell solution in a 15-ml centrifuge tube and centrifuge for 5 min at 800 × *g*, 4°C. Decant the supernatant. The cell pellet can now be processed for membrane and cytosolic NAALADase, or alternatively stored at –80°C for up to 3 months for future use.

Task 5 (Months 9 – 30): In vivo and PET/CT imaging evaluation of the synthesized theranostic agents (Sun)

Currently ongoing. No data yet.

KEY RESEARCH ACCOMPLISHMENTS

- Enantiopure bifunctional chelators (BFCs) were designed for radiopharmaceuticals
- The chirality effect of BFCs was evaluated on integrin $\alpha_v\beta_3$ targeted agents
- Negligible effect of BFC chirality was observed by *in vitro* and *in vivo* evaluations
- BFC chirality may play a role in other receptor targeted radiopharmaceuticals
- A theranostic drug conjugate for prostate cancer was designed and synthesized with the integration of a PET imaging functionality.

REPORTABLE OUTCOMES

1. Singh AN, Dakanali M, Hao G, Ramezani S, Kumar A, Sun X: Enantiopure bifunctional chelators for copper radiopharmaceuticals - Does chirality matter in radiotracer design? *Eur. J. Med. Chem.* **2014**, 80, 308-315.
2. Lo S-T, Kumar A, and Sun X: Delivery and Controlled Release of Therapeutics via Dendrimer Scaffolds. A book chapter of "*Nanoparticle Delivery of Biotherapeutics*" edited by Vooght-Johnson. Published by Future Science Group, **2014**, in press

CONCLUSION

Three enantiopure BFC scaffolds for copper radiopharmaceuticals were designed, synthesized and evaluated using a well-validated integrin $\alpha_v\beta_3$ ligand. Our work suggests that the chirality of BFC scaffolds plays an insignificant role in integrin $\alpha_v\beta_3$ targeted copper radiopharmaceuticals. Although this observation does not support our design rationale, the importance of BFC chirality in radiopharmaceutical agents cannot be undervalued without discretion when it is applied to other biological targets. The theranostic MDC design would enable concurrent prostate cancer treatment and real-time monitoring, which can provide insights for clinical evaluation in terms of the drug delivery kinetics, local response, and overall efficacy. Such design will be modified and incorporated into the dendrimeric platforms to accomplish further Aims in this project.

REFERENCES:

1. Cooke, R.C., et al., *Odor Detection Thresholds and Enantiomeric Distributions of Several 4-Alkyl Substituted gamma-Lactones in Australian Red Wine.* Journal of Agricultural and Food Chemistry, 2009. **57**(6): p. 2462-2467.
2. Levy, S.G., et al., *Development of a Multigram Asymmetric Synthesis of 2-(R)-2-(4,7,10-Tris tert-Butylcarboxymethyl-1,4,7,10-tetraazacyclododec-1-yl)-pentanedioic Acid, 1-tert-Butyl Esterg (R)-tert-Bu-4-DOTAGA.* Organic Process Research & Development, 2009. **13**(3): p. 535-542.
3. Zhang, X.Z., et al., *Quantitative PET imaging of tumor integrin alpha(v)beta(3) expression with F-18-FRGD2.* Journal of Nuclear Medicine, 2006. **47**(1): p. 113-121.
4. Wong, E.H., et al., *Synthesis and characterization of cross-bridged cyclams and pendant-armed derivatives and structural studies of their copper(II) complexes.* Journal of the American Chemical Society, 2000. **122**(43): p. 10561-10572.
5. Liu, W., et al., *Imparting Multivalency to a Bifunctional Chelator: A Scaffold Design for Targeted PET Imaging Probes.* Angewandte Chemie-International Edition, 2009. **48**(40): p. 7346-7349.

6. Maresca, K.P., et al., *A series of halogenated heterodimeric inhibitors of prostate specific membrane antigen (PSMA) as radiolabeled probes for targeting prostate cancer.* J Med Chem, 2009. **52**(2): p. 347-57.
7. Scott, P.J.H. and X. Shao, *Fully automated, high yielding production of N-succinimidyl 4-[F-18]fluorobenzoate ([F-18]SFB), and its use in microwave-enhanced radiochemical coupling reactions.* Journal of Labelled Compounds & Radiopharmaceuticals, 2010. **53**(9): p. 586-591.
8. Thonon, D., et al., *Fully Automated Preparation and Conjugation of N-Succinimidyl 4-[F-18]Fluorobenzoate ([F-18]SFB) with RGD Peptide Using a GE FASTlab (TM) Synthesizer.* Molecular Imaging and Biology, 2011. **13**(6): p. 1088-1095.
9. Kang, S.O., V.W. Day, and K. Bowman-James, *The Influence of Amine Functionalities on Anion Binding in Polyamide-Containing Macrocycles.* Organic Letters, 2009. **11**(16): p. 3654-3657.